Applied Geochemistry 130 (2021) 104978

Contents lists available at ScienceDirect

Applied Geochemistry

journal homepage: www.elsevier.com/locate/apgeochem

Method for analyzing the oxygen isotope composition of HCl-extractable inorganic phosphate in sediments and soils

Yong Liu [a,b,c], Jingfu Wang [a,c,*], Haiquan Yang [a,c,**], Shihao Jiang [a,d], Zuxue Jin [a,c], Jingan Chen [a,c]

[a] State Key Laboratory of Environmental Geochemistry, Institute of Geochemistry, Chinese Academy of Sciences, Guiyang, 550081, China
[b] College of Biological and Environmental Engineering, Guiyang University, Guiyang, 550005, China
[c] University of Chinese Academy of Sciences, Beijing, 100049, China
[d] School of Earth Sciences, China University of Geosciences, Wuhan, 430074, China

ARTICLE INFO

Keywords:
Method
Phosphate oxygen isotope
HCl-P_{TI}
Zr-oxide gel
Sediments
Soils

ABSTRACT

The oxygen isotope ratio in phosphate ($\delta^{18}O_P$) is an effective tool for tracing the sources of phosphorus (P) and their biogeochemical cycles. The HCl-extractable inorganic phosphate (HCl-P_{TI}) is the primary component of P and plays a key role in the dynamic transformation of P in sediment and soil. However, it has always been difficult to purity sample for analyzing the $\delta^{18}O_P$ composition of HCl-P_{TI} due to the significantly interference of large amounts of $Fe^{2+/3+}$, Ca^{2+}, Cl^- and other impurities in the HCl-P_{TI} extracts. In this study, we developed a simple and promising purification method for $\delta^{18}O_P$ analysis of HCl-P_{TI} in sediments and soils based on the superior selective enrichment and elution abilities of phosphate (PO_4) and efficient synchronous removal of impurities by Zr-Oxide gel in highly acidic HCl-P_{TI} extract. The enrichment rate and elution rate of PO_4 in the HCl-P_{TI} extract by the Zr-Oxide gel could achieve 100% respectively, and the synchronous removal rates of most anions, dissolved organic carbon (DOC), metals, and trace elements could be above 96% respectively, reducing the tedious operation of conventional methods and the difficulties in removal of impurities, such as Cl^- in HCl-P_{TI} extract. It's indicated that the purity of the Ag_3PO_4 solid for $\delta^{18}O_P$ composition analysis of HCl-P_{TI} could reach 99.9%. The above results show that the new method is very simple, efficient and reliable for the $\delta^{18}O_P$ analysis of HCl-P_{TI} in sediments and soils. This study provides new methodological support for identifying the sources of P and tracing their biogeochemical cycles in sediment or soil environment.

1. Introduction

Phosphorus (P) is a basic nutrient element to constitute the life material, such as the component of cell membrane structure, genetic material (DNA) and energy material (ATP) of organisms, a key nutrient that affects the growth and development of organisms, and an important driving factor of water primary productivity. In nature, P is mainly bound to oxygen (O) and widely as inorganic phosphate (PO_4, i.e., PO_4^{3-}, HPO_4^{2-} and $H_2PO_4^-$) found in sediments and soils, and often has different bioavailability under different sediment or soil background condition, playing a key role in the dynamic transformation of P (Reina et al., 2006; Zhang et al., 2020; Pu et al., 2020). For instance, rock weathering or artificial fertilization first provide the soil with a large amount of PO_4, which becomes the most important nutrient required by biology to participate in the migration, transformation and biological recycling of P in the soil (Walker and Syers, 1976; Bate et al., 2008; Tamburini et al., 2012; Helfenstein et al., 2018; Koch et al., 2018; Ishida et al., 2019). One another, with the leaching of soil and the discharge of P-containing wastewater from human activities, sediments, as an important sink of P, store large amounts of PO_4 in water or from terrestrial sources and well record their historical deposition process, and can also release PO_4 to the overlying water with the change of environmental conditions, which becomes the key circulation part of water P and has an important influence on lake eutrophication (Jin et al., 2006; Kwak et al., 2018; Chen et al., 2019; Ezzati et al., 2020; Guo et al., 2020).

P has only one stable isotope (^{31}P) and cannot be used as a stable isotopic tracer, while O has three stable isotopes (^{16}O, ^{17}O and ^{18}O). P–O bond in PO_4 is highly resistant to inorganic hydrolysis and can be broken

* Corresponding author. State Key Laboratory of Environmental Geochemistry, Institute of Geochemistry, Chinese Academy of Sciences, Guiyang, 550081, China.
** Corresponding author. State Key Laboratory of Environmental Geochemistry, Institute of Geochemistry, Chinese Academy of Sciences, Guiyang, 550081, China.
E-mail addresses: wangjingfu@vip.skleg.cn (J. Wang), yanghaiquan@vip.skleg.cn (H. Yang).

https://doi.org/10.1016/j.apgeochem.2021.104978
Received 21 February 2021; Received in revised form 10 April 2021; Accepted 21 April 2021
Available online 27 April 2021
0883-2927/

under the action of biology or enzyme to exchange O isotope with the surrounding water molecules, so the O isotope ratio in PO_4 ($\delta^{18}O_P$) can be an effective tracer to identify the sources of P and their biogeochemical cycles (Longinelli et al., 1973; Blake et al., 1997; Paytan et al., 2002; McLaughlin et al., 2004, 2006, 2013; Liang and Blake, 2006, 2009; Goldhammer et al., 2011; Gooddy et al., 2015; Mingus et al., 2019; Pfahler et al., 2020). Chang and Blake (2015) developed the equilibrium equation1000 lna (PO4 − H2O) = 14.43 *1000/T(K) − 26.54, to evaluate the biogeochemical cycle of P. The $\delta^{18}O_P$ has been used to trace the sources of P and their biogeochemical cycle in sediments and soils. Firstly, the $\delta^{18}O_P$ can trace the historical sources of P and their biogeochemical behavior in sediments, thus evaluating the potential ecological effects on aquatic ecosystems (Jaisi et al., 2010, 2011; Paytan et al., 2017; Liu et al., 2019; Yuan et al., 2019). Secondly, the $\delta^{18}O_P$ can trace the P sources and their transport and transformation in the soils for analyzing the PO_4 absorption and utilization capacity of plants and plant rhizosphere micro-ecosystems activity (Tamburini et al., 2012, 2014; Pistocchi et al., 2017; Joshi et al., 2018; Granger et al., 2017; Bi et al., 2018; Tian et al., 2020). Besides, the $\delta^{18}O_P$ can also systematically reveal geochemistry and climatic change information, such as sediment-soil rock weathering, transportation, etc (Blake et al., 2010; Burmann et al., 2013; Ishida et al., 2019; Ide et al., 2020). Researchers have used HCl solution to extract the HCl-extractable inorganic phosphate (HCl-P_{TI}) from sediment or soil samples (Tamburini et al., 2010; Zohar et al., 2010; Amelung et al., 2015; Granger et al., 2017; Liu et al., 2019). For calcareous sediments or soils, the HCl-P_{TI} is mainly the calcium-bound P (Ca-P_I) dominated by hydroxyapatite with low bioavailability, and thus the $\delta^{18}O_P$ composition retains the original information of apatite diagenesis (Angert et al., 2012; Paytan et al., 2017). For acidic sediments or soils with a light texture, the HCl-P_{TI} is mainly iron/aluminum-bound P (Fe/Al-P_I) with high bioavailability, and the $\delta^{18}O_P$ composition more reflects the dynamic transformation behavior of P, such as the biological utilization of P as a nutrient in sediments or soils (Tamburini et al., 2012; Pistocchi et al., 2017).

However, the purification method for $\delta^{18}O_P$ analysis of HCl-P_{TI} in sediment or soil sample has always been complicated because the HCl-P_{TI} extract contains a large number of impurities, such as $Fe^{2+/3+}$, Ca^{2+} and other metal impurities, mainly synchronously extracted from the sediment or soil samples, as well as large amounts of Cl^-, mainly from the HCl extractant itself, which cause considerable interference for the purification operations and the final purity of Ag_3PO_4 solid for $\delta^{18}O_P$ composition analysis (Zohar et al., 2010; Liu et al., 2019). Although the $\delta^{18}O_P$ methodology has been developed rapidly and applied successfully and widely, the conventional methods have several limitations. For instance, Tamburini et al., (2010) extracted HCl-P_{TI} from 20 to 25 g dry soil using 1 M HCl, removed the organic matters and cations by multi-step chemical precipitation reactions, such as ammonium phosphomolybdate (APM) and magnesium ammonium phosphate (MAP), and anion/cation exchange resin, respectively, and finally the Ag_3PO_4 solid was formed for $\delta^{18}O_P$ composition analysis. However, a large soil sample weight was utilized in the method, resulting in a high proportion of total impurities and significantly increasing the difficulty of the $\delta^{18}O_P$ purification. Similarly, Weiner et al., (2011) used the anion exchange resin to enrich and elute the dissolved phosphate (DIP) in the soil and the DAX macroporous resin to remove organic matters to form $CePO_4$ precipitation, and then the cation exchange resin to remove Ce^{3+} and finally to form the Ag_3PO_4 solid for $\delta^{18}O_P$ composition analysis. Although this method was employed to extract the DIP for direct utilization by organisms, the total amount of PO_4 obtained in the extract was relatively small, and it is difficult to meet the $\delta^{18}O_P$ purification for the samples with low PO_4 content. Zohar et al. (2010) and Liu et al. (2019) established methods for the $\delta^{18}O_P$ purification of different P fractionations in soils and sediments, respectively. However, it's relatively complicated for the principle of multi-step removal of various impurities and passive continuous purification and concentration of PO_4 from the sediment or soil extracts.

Zr-Oxide gel, used in the primary component of diffusive gradients in thin films (DGT) technique, is a gel bond phase prepared by mixing semi-dry amorphous zirconium hydroxide and acrylamide solution and is widely adopted for *in situ* high resolution analysis of P concentration in water (Ding et al., 2010, 2011). Accumulating studies have shown that the Zr-Oxide gel has a highly selective enrichment of PO_4 but is less affected by coexisting anions and cations, especially its enrichment ability can significantly enhance due to the lower solution pH in acidic solution systems, and PO_4 can be easily eluted from the Zr-Oxide gel in alkaline conditions (Chitrakar et al., 2006; Ding et al., 2010, 2011). In addition, as a kind of thin-layer gel phase material, compared with many other PO_4-enriched chemicals, Zr-Oxide gel has advantages in the operation of concentration and separation of PO_4 from solution. Considering the above characteristics, Zr-Oxide gel was used in the $\delta^{18}O_P$ purification for HCl-P_{TI} of sediments and soils in this study and developed a novel and simple method for $\delta^{18}O_P$ analysis. The established method effectively overcame the limitations of complex chemical components of the HCl-P_{TI} extract as well as the tedious and complicated operations of conventional methods. This study provides a reliable methodology for identifying the sources of P and tracing their biogeochemical cycles in sediment or soil environment, and also provides insights into the use of different materials for the $\delta^{18}O_P$ analysis methods in environmental systems with complex chemical compositions.

2. Materials and methods

2.1. Main materials

The main reagents and materials used in this study were resourced as follows: Zr-Oxide gel (Easy Sensor Ltd., Nanjing, China; www.easysensor.net; diameter of 2.5 cm and total area of 4.90 cm^2), cerium nitrate hexahydrate ($Ce(NO_3)_3 \bullet 6H_2O$, 99.5%, Sigma-Aldrich, America), silver nitrate ($AgNO_3$, 99.9+%, Alfa Aesar, America), 50-ml centrifuge tube (light-colored from Corning, Germany; black-colored from Greiner, Germany), cation exchange resin (Biorad AG 50W-X8, America), potassium acetate (KAc, GR, Aladdin, China), and hydrochloric acid (HCl, GR), nitric acid (HNO_3, GR), acetic acid (HAc, GR), ammonium hydroxide (NH_4OH, GR), hydrogen peroxide (H_2O_2, GR) and sodium hydroxide (NaOH, GR) from Sinopharm Chemical Reagent Company, China.

2.2. Sample collection

From May to August in 2019, the surface sediments were collected from the south (DCS), center (DCC), and Guanyin (DCG) sites of Dianchi Lake in Yunnan province, China, the Jinzhong (AHJ) and Youyu (AHY) sites of Aha Lake in Guizhou province, China. The surface soil samples were collected at GHS, GHX, GBL and GLD sites in the agricultural non-point source pollution area of Kelan Reservoir in Guangxi province, China (Fig. 1). The sediment and soil samples were freeze-dried to remove large particles and ground to below 200 mesh for chemical analysis.

2.3. HCl-P_{TI} extraction and impurity removal experiments

Accurately 3.3 g of sediment or soil samples were mixed with 200 ml of 1 M HCl and continuously shaken for 16 h. Then this mixture was passed through a 0.45 μm filter membrane to obtain the HCl-P_{TI} extract. The HCl-P_{TI} extract of sediment obtained from the AHJ site was taken as an example: 5 ml of HCl-P_{TI} extract was taken to determine the concentration of common anions, DOC, heavy metals, and trace elements. Five discs of Zr-Oxide gels were placed into the remaining 195 ml extract, shaken continuously for 5 days, then the Zr-Oxide gels were taken out and placed in 20 ml 1 M NaOH and shaken continuously for 24 h to elute PO_4, and finally passed through a 0.45 μm filter membrane to obtain the PO_4 eluent and analyze the concentrations of common anions,

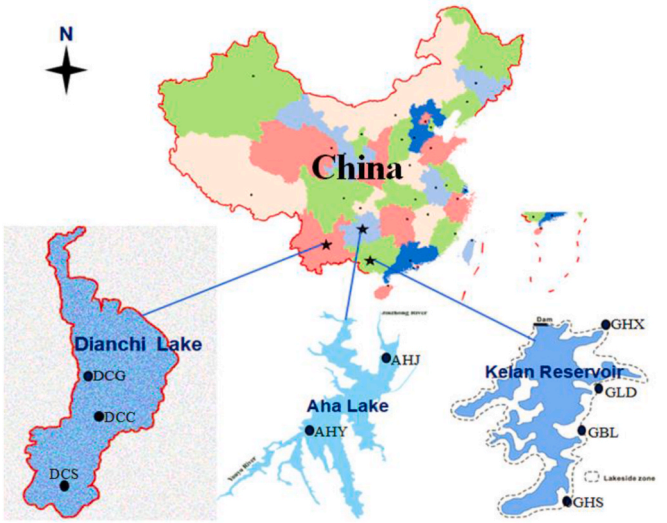

Fig. 1. Distribution of collection sites for the sediment and soil samples in different lake regions.

cations, DOC, metals, and trace elements. The impurity removal was quantified by comparing the difference between the concentration of various ions before and after the Zr-Oxide gels treatment.

2.4. The purification protocol for $\delta^{18}O_P$ analysis of HCl-P_{TI}

The purification protocol for $\delta^{18}O_P$ analysis of HCl-P_{TI} in sediment and soil samples is shown in Fig. 2. The specific operation steps were as follows:

1) Enrichment and elution of PO_4 by Zr-Oxide gel

The Zr-Oxide gels were placed to continuously enrich PO_4 of the HCl-P_{TI} extract for a few days. The number of gels and standing times are listed in Table 1. After enrichment of PO_4, the surface of Zr-Oxide gels (containing PO_4) was washed with pure water and placed in a 50 ml centrifuge tube, 1 M NaOH (according to 4 ml of 1 M NaOH per gel) was added, shaken continuously for 24 h, and then passed through a 0.45 μm filter membrane to obtain PO_4 eluent.

2) Formation of $CePO_4$ precipitation to remove Cl^-

The pH of the PO_4 eluent was adjusted to 5.8 with 5 M HNO_3, then 2 ml of Ce^{3+} solution (0.5 g of $Ce(NO_3)_3 \bullet 6H_2O$ in 2 ml pure water) was added, and the pH was adjusted back to 5.5 with 1 M KAc to obtain the milky white $CePO_4$ precipitate, which was then centrifuged at 4000 r/min for 15 min and washed 3 times using 5 ml of prepared KAc-HAc buffer solution (pH 5.6; added 2 drops of pure HAc to 1 L of pure water, and then adjusted the pH to 5.6 with 1 M KAc) to completely remove the residual Cl^- on the surface of $CePO_4$ precipitate (In fact, very little Cl^- remained, Table S2). The Cl^- can be detected with dilute $AgNO_3$ solution.

3) Removal of Ce^{3+}, Zr^{4+} and other cations using cation exchange resin

The $CePO_4$ precipitate was completely dissolved with 15 ml of 0.2 M HNO_3. Then, 5 ml of Biorad AG 50W-X8 cation exchange resin was added and continuously shaken overnight to remove cations, such as Ce^{3+} and Zr^{4+}. After passing through a 0.45 μm filter membrane, the residual PO_4 on the resin surface was rinsed with pure water and also directly filtered into a 50 ml black centrifuge tube to obtain PO_4 filtrate.

4) Formation of Ag_3PO_4 precipitation and its further purification

The pH of above filtrate was adjusted with 2.8% NH_4OH solution to 8.0, then 2 ml of Ag^+ solution (0.5 g of $AgNO_3$ in 2 ml of pure water) was added to obtain a light yellow Ag_3PO_4 precipitate, left overnight, and the supernatant was discarded after centrifugation at 4000 r/min, 15 min. The Ag_3PO_4 precipitate was washed 3 times with pure water, 5 ml of 15% H_2O_2 (adjusted the pH to 7.3 with a small amount of ammonia) was added, left for 3 h to remove residual organic matters, and then the supernatant was discarded after centrifugation. The Ag_3PO_4 precipitate was again washed with 10 ml of pure water for 3 times. It should be cautious to carry out above operations to prevent the loss of Ag_3PO_4 precipitate. Finally, it was freeze-dried or dried at 50 °C to obtain the high-purity Ag_3PO_4 solid for $\delta^{18}O_P$ composition analysis.

2.5. Analysis and test

The soluble reactive P (SRP) concentration in HCl-P_{TI} extract and PO_4 eluent was measured using the molybdenum antimony colorimetric method (Murphy and Riley, 1962). The concentration of anion and cation were measured using ion chromatography (ICS-90, DIONEX, America) and plasma atomic emission spectrometer (ICP-AES) (Vista Mpx, VARIAN, America), respectively. Total organic carbon (TOC) was measured using a total organic carbon/nitrogen analyzer (High TOCII, Elementar, Germany). The chemical composition of the prepared

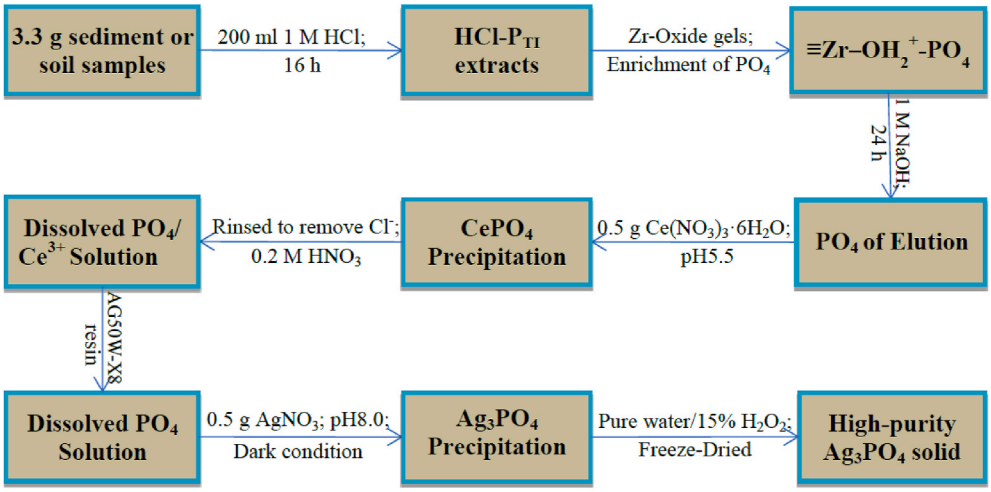

Fig. 2. Purification protocol for $\delta^{18}O_P$ analysis of HCl-P_{TI} in sediments and soils.

Table 1
The enrichment and elution of PO_4 in HCl-P_{TI} extract by Zr-Oxide gel.

Site	Type	PO_4 amounts in extract μg	Gel number	Days of gel placed	PO_4 amounts in supernatant after enrichment μg	PO_4 amount on gels μg	PO_4 amount in eluent μg	PO_4 amount per gel μg	PO_4 amount per unit area gel μg/cm^2	Enrichment rate of PO_4%	Elution rate of PO_4%	PO_4 recovery %	n
DCS	Sediment	5310.7 ± 184.6	5	5	740.1 ± 30.3	4570.6 ± 155.7	4397.6 ± 106.4	879.5 ± 21.3	179.3 ± 4.3	86.1 ± 0.2	96.3 ± 5.6	96.9 ± 4.8	3
DCC	Sediment	2626.7 ± 51.5	5	3	164.1 ± 10.5	2462.6 ± 43.8	2353.0 ± 57.8	470.6 ± 11.6	95.9 ± 2.4	93.8 ± 0.3	95.6 ± 3.9	95.9 ± 3.7	4
DCG	Sediment	2946.7 ± 23.0	5	5	176.2 ± 8.0	2770.4 ± 24.5	2539.3 ± 185.1	507.9 ± 37.0	103.5 ± 7.5	94.0 ± 0.3	91.6 ± 6.0	92.1 ± 5.6	3
AHJ	Sediment	584.4 ± 58.3	3	3	12.4 ± 7.5	572.0 ± 50.8	552.3 ± 117.1	184.1 ± 39.0	37.5 ± 8.0	97.9 ± 1.1	97.9 ± 9.2	97.8 ± 9.1	3
AHY	Sediment	565.3 ± 41.7	3	3	54.3 ± 6.3	511.1 ± 47.8	467.9 ± 10.5	156.0 ± 3.5	31.8 ± 0.7	90.3 ± 1.9	95.2 ± 8.1	95.6 ± 7.4	3
GHS	Soil	718.9 ± 43.2	3	3	40.4 ± 3.2	678.5 ± 43.3	662.5 ± 27.0	220.8 ± 9.0	45.0 ± 1.8	94.4 ± 0.6	98.1 ± 10.0	98.1 ± 9.5	3
GHX	Soil	892.2 ± 60.8	3	3	65.6 ± 14.8	826.6 ± 74.5	824.6 ± 15.0	274.9 ± 5.0	56.0 ± 1.0	92.6 ± 2.2	100.4 ± 10.6	100.2 ± 9.7	3
GBL	Soil	758.3 ± 16.5	3	3	40.8 ± 15.3	717.5 ± 18.4	710.6 ± 13.7	236.9 ± 4.6	48.3 ± 0.9	94.6 ± 2.0	99.1 ± 1.9	99.1 ± 1.8	3
GLD	Soil	388.9 ± 36.6	3	3	18.2 ± 10.6	370.7 ± 26.0	366.6 ± 22.9	122.2 ± 7.6	24.9 ± 1.6	95.5 ± 2.4	99.4 ± 11.7	99.6 ± 11.1	3
GHX2	Soil	824.8 ± 3.1	5	5	/	824.8 ± 3.1	801.1 ± 10.2	160.2 ± 2.0	32.7 ± 0.4	100.0 ± 0.0	97.1 ± 0.9	97.1 ± 0.9	3
GLD2	Soil	338.7 ± 21.6	5	5	/	338.7 ± 21.6	340.5 ± 37.6	68.1 ± 7.5	13.9 ± 1.5	100.0 ± 0.0	100.4 ± 7.0	100.4 ± 7.0	3

Note: PO_4 amount on gels = PO_4 amount in extract - PO_4 amount in supernatant after enrichment; Enrichment rate of PO_4% = PO_4 amount on gels/PO_4 amount in extract *100%; Elution rate of PO_4% = PO_4 amount in eluent/PO_4 amount on gels*100%; PO_4 recovery % = (PO_4 amount in eluent + PO_4 amount in supernatant after enrichment)/PO_4 amount in extract * 100%; "/" means below the detection limit; GHX2 and GHX, GLD2 and GLD are the same sample with HCl-P_{TI} extracted in two batches, respectively.

Ag_3PO_4 solid sample was analyzed using X-Ray Diffraction (XRD) (Empyrean, PANalytical BV, Holland) and scanning electron microscope (SEM) (Institute of Geochemistry, Chinese Academy of Sciences). The $\delta^{18}O_P$ composition of the Ag_3PO_4 solid sample (reacted to form CO at 1380 °C) was determined using the gas isotope ratio mass spectrometer (MAT253, Thermo Scientific, America) of the Third Institute of Oceanography of the State Oceanic Administration. The $\delta^{18}O_P$ isotope value was standardized using the Vienna standard average ocean water oxygen $^{18}O/^{16}O$. The analysis accuracy was better than 0.3‰, and international Ag_3PO_4 standard (21.7‰, B2207, EMA, UK) was used for testing and calibration.

3. Results

3.1. HCl-P_{TI} contents in sediment and soil samples

The HCl-P_{TI} contents in the sediment and soil samples are depicted in Fig. 3. The sediment HCl-P_{TI} contents of DCS, DCC, and DCG sites in Dianchi Lake were 1609.3 μg/g, 796.0 μg/g, and 892.9 μg/g, respectively. The sediment HCl-P_{TI} contents of the AHJ and AHY sites in Aha Lake were 177.1 μg/g and 171.3 μg/g, respectively. The soil HCl-P_{TI} contents of GHS, GHX, GBL, and GLD sites in the agricultural non-point source pollution area of Kelan Reservoir were 217.9 μg/g, 270.4 μg/g, 229.8 μg/g, and 117.8 μg/g, respectively. The SRP concentration in the HCl-P_{TI} extract is vital for the subsequent $\delta^{18}O_P$ purification of sample. The SRP concentrations in the sediment HCl-P_{TI} extracts of Dianchi Lake and Aha Lake were 13,133.6–26,553.5 μg/L and 2826.7–2922.0 μg/L, respectively, while the SRP concentration range of HCl-P_{TI} extracts in the soils of the agricultural non-point source pollution area of Kelan Reservoir was 1944.4–4460.9 μg/L. The above results confirmed that the selected sediment and soil samples had a wide range of HCl-P_{TI} content, and thus these samples were considered as the objects to the study on the purification protocol for $\delta^{18}O_P$ analysis.

3.2. Enrichment and elution of PO_4 in HCl-P_{TI} extracts by Zr-Oxide gel

With the increase of enrichment time by Zr-Oxide gels, the SRP concentrations in HCl-P_{TI} extracts decreased sharply with the time of

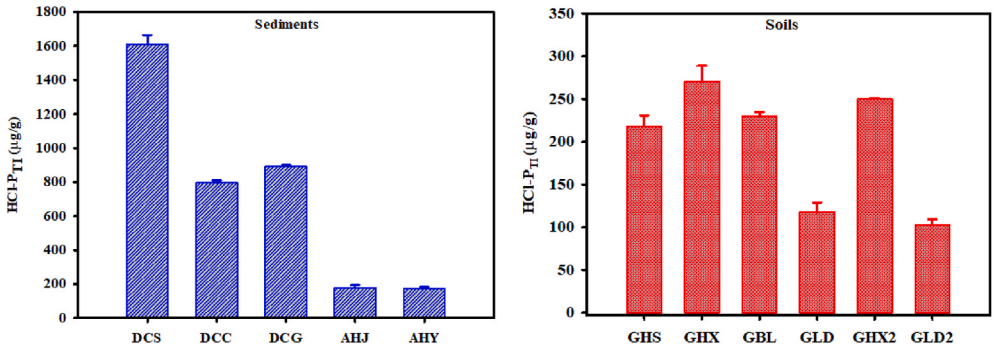

Fig. 3. HCl-P_{TI} contents of sediment and soil samples at different sitesNote
GHX2 and GHX, GLD2 and GLD are the data of HCl-P_{TI} extracted in two batches in the same sample (n = 3).

PO_4 enrichment by Zr-Oxide gels (Fig. 4). Within 5 days, the SRP concentration in the sediment HCl-P_{TI} extract obtained from DCS and DCG sites of Dianchi Lake decreased from 26,553.5 μg/L to 3700.5 μg/L, and 14,733.3 μg/L to 877.9 μg/L, respectively, and the PO_4 enrichment rates were 86.1% and 94.0%, respectively; Within 3 days, the SRP concentration in the sediment HCl-P_{TI} extracts obtained from AHJ and AHY sites of Aha Lake decreased from 2922.0 μg/L to 62.1 μg/L, and 2826.7 μg/L to 271.3 μg/L, respectively, and the PO_4 enrichment rates were 97.9% and 90.3%, respectively. The SRP concentration in the soil HCl-P_{TI} extracts obtained from the GHS, GHX, GBL and GLD sites of the agricultural non-point source pollution area of Kelan Reservoir decreased from 3594.7 μg/L to 202.0 μg/L, 4460.9 μg/L to 328.1 μg/L, 3791.5 μg/L to 204.2 μg/L, and 1944.4 μg/L to 90.8 μg/L, and the PO_4 enrichment rates were 94.4%, 92.6%, 94.6%, and 95.5%, respectively. Significantly, within 4 days, the SRP concentration in the soil HCl-P_{TI} extracts obtained from GHX2 and GLD2 sites dropped from 4124.0 μg/L and 1693.7 μg/L to 0, and the PO_4 enrichment rates were 100%, respectively.

As summarized in Table 1, the total amount of PO_4 eluted from the Zr-Oxide gel of sediment HCl-P_{TI} extracts from DCS, DCC and DCG sites of Dianchi Lake ranged from 2539.3 to 4397.6 μg P (calculated as P, the same below), with the elution rate 91.6–96.3%, and the amount of PO_4 per unit area gel was 95.9–179.3 μg P/cm^2. In the HCl-P_{TI} extract of the Aha Lake sediments, the total amount of PO_4 eluted from the Zr-Oxide gel was 467.9 μg P and 552.3 μg P, respectively, with the elution rate of 95.2–97.9%, and the amount of PO_4 per unit area gel was 31.8–37.5 μg P/cm^2. In the soil HCl-P_{TI} extract of GHS, GHX, GBL, GLD sites of Kelan Reservoir, the total amount of PO_4 eluted from the Zr-Oxide gel was 340.5–824.6 μg P, with the elution rate 97.1–100.4%, and the amount of PO_4 eluted from per unit area gel was 13.9–56.0 μg P/cm^2. In the process of PO_4 enrichment and elution by the Zr-Oxide gel, the recovery rate of PO_4 in the sample was between 92.1% and 100.2%.

3.3. Simultaneous removal for impurities in HCl-P_{TI} extracts by Zr-Oxide gel

The HCl-P_{TI} extract contained a large number of common anions, DOC, different metals, trace elements, and other impurities (Table S1). The concentrations of Cl^-, SO_4^{2-}, Na, Fe, and Ca were 35,500.0 mg/L, 157.8 mg/L, 165.2 mg/L, 409.6 mg/L, and 673.5 mg/L, respectively. However, the concentrations of various impurities in the PO_4 eluent significantly reduced compared with the HCl-P_{TI} extract, and the concentrations of many impurities were very low or below the detection limit, thus, they were not included in the statistics (Table S2). The impurities with relatively larger amounts in the eluent were Cl^-, SO_4^{2-}, DOC, Fe, and Ca, which were only 2.6 mg, 4.2 mg, 0.2 mg, 10 μg, and 10 μg, respectively. Apart from the lower removal rate of K (71.6%), Zr-Oxide gel had a removal rate of more than 99.7% for most metals and trace elements, up to 98.3% for DOC, and more than 96.2% for main anions (for SO_4^{2-} was slightly lower, which was 85.9%). The total amount of Zr in HCl-P_{TI} extract was very small (~1 μg), but slightly higher (20 μg) in the PO_4 eluent, which was probably introduced by the Zr-Oxide gel itself during the PO_4 elution.

3.4. The purity of Ag_3PO_4 solid sample analysis

The chemical composition of the Ag_3PO_4 solid sample obtained by the $\delta^{18}O_P$ purification protocol of HCl-P_{TI} with Zr-Oxide gel was analyzed using SEM and XRD (Fig. 5). SEM analysis demonstrated that the Ag_3PO_4 solid had no other impurities except Ag, P and O. The At% of P and Ag were 10.14 and 30.01, respectively, combined with the atomic ratio of these two in pure Ag_3PO_4 to be 1:3, so the purity of the Ag_3PO_4 solid sample could be estimated to reach 99.9%. The XRD analysis confirmed that the obtained Ag_3PO_4 solid sample was of high purity with relatively small amount of Ag, which might have happened due to the photolysis reaction of Ag_3PO_4 or the reduction of Ag^+ from $AgNO_3$ solution (Liu et al., 2019). However, in the $\delta^{18}O_P$ composition test, the presence of a small amount of Ag did not affect its test accuracy (Liu et al., 2021).

3.5. The $\delta^{18}O_P$ compositions of HCl-P_{TI} in sediment and soil samples

As depicted in Fig. 6, the $\delta^{18}O_P$ compositions of HCl-P_{TI} in sediment and soil samples from the three different regions significantly differed, indicating the differences in the sources and biogeochemical characteristics of P in sediments or soils from different regions. The $\delta^{18}O_P$ compositions of HCl-P_{TI} in the sediments of Dianchi Lake were relatively negative, ranging from 15.2‰ to 16.7‰, combined with the sampling

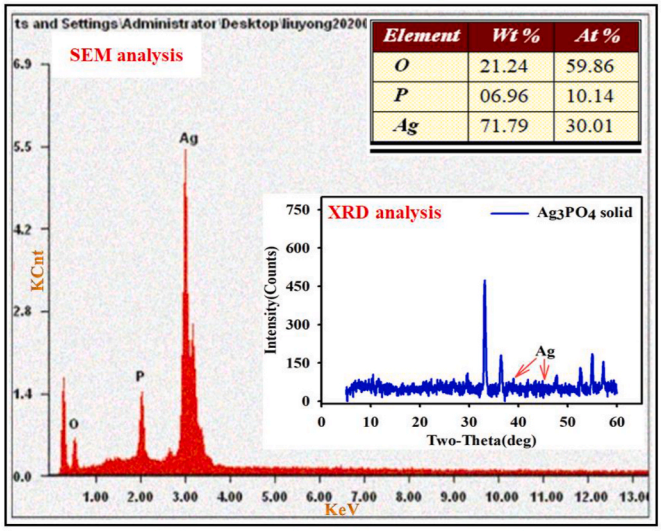

Fig. 5. Purity of Ag_3PO_4 solid sample analysis obtained from HCl-P_{TI} (SEM and XRD analysis).

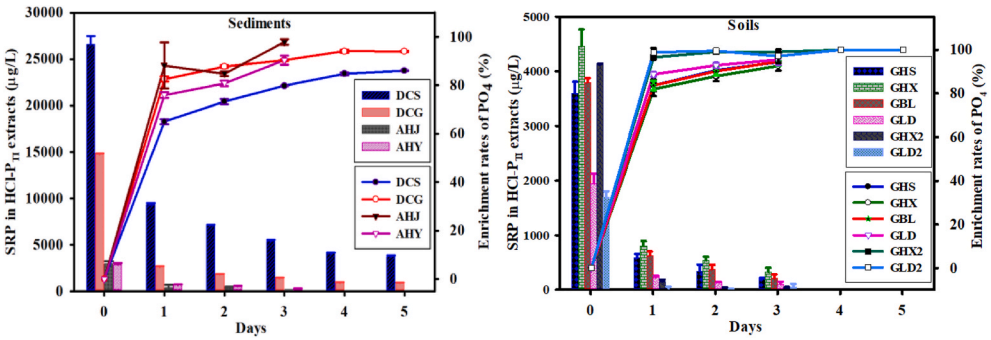

Fig. 4. Changes of SRP concentrations in HCl-P_{TI} extracts and PO_4 enrichment rates by Zr-Oxide gel.

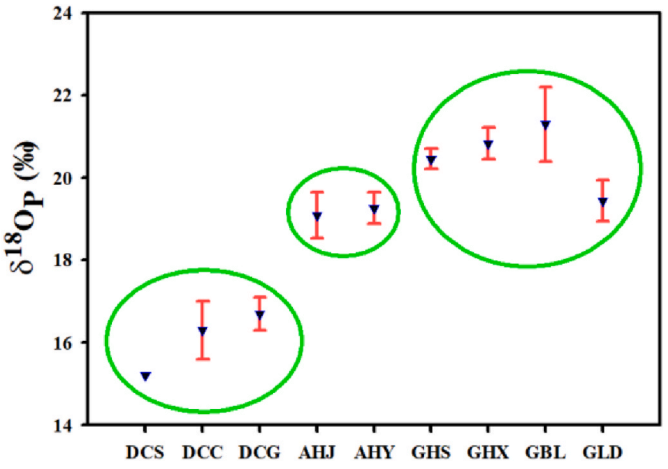

Fig. 6. $\delta^{18}O_P$ compositions of HCl-P_{TI} in sediment and soil samples from different lake regions.

sites of these samples are surrounded by large-scale P deposits and the Ca-P_I in the sediments of Dianchi Lake is generally high (Zhu et al., 2017), indicating the $\delta^{18}O_P$ compositions of sediment HCl-P_{TI} are more representative of existence of inactive apatite, such as Ca-P_I. At two estuary sites of Aha Lake with high microbial activity (Wang et al., 2003), the $\delta^{18}O_P$ compositions of sediment HCl-P_{TI} was 19.1‰ and 19.3‰, indicating the existence of P with high biological activity, such as Fe/Al-P_I, which is also consistent with previous studies (Sun et al., 2017). The $\delta^{18}O_P$ compositions of soil HCl-P_{TI} in the buffer zone of agriculture (planting areas of sugarcane, rice, fruit, etc.) and lakeside wetland remained positive between 19.5‰ and 21.3‰. In agricultural areas, the bioavailability of the HCl-P_{TI} component is higher, so higher biological modification of $\delta^{18}O_P$ composition is possible. In this area, soil $NaHCO_3$–P and NaOH–P account for 55.1% of the total phosphorus (TP), and inactive Ca-P_I accounts for less than 2% (Wang et al., 2020). Therefore, the $\delta^{18}O_P$ compositions of soil HCl-P_{TI} mainly indicated the signal of the biogeochemical cycle of soil P, such as labile and weakly adsorbed P.

According to the deviation of the $\delta^{18}O_P$ composition of HCl-P_{TI} from the equilibrium value of $\delta^{18}O_{EQ}$, it can be evaluated whether the $\delta^{18}O_P$ composition indication is based on P source or biological cycle of P (Longinelli et al., 1973; Chang and Blake, 2015). Unfortunately, the sediment and soil pore water samples were not collected and the $\delta^{18}O_w$ composition of pore water wasn't analyzed in this study, thus, the theoretical equilibrium value of $\delta^{18}O_{EQ}$ could not be calculated.

4. Discussion

4.1. Effect of Zr-Oxide gel on enrichment and elution of PO_4 in HCl-P_{TI} extracts

The content of HCl-P_{TI} in sediments and soils selected in this study was quite different, ranging from 117.8 to 1609.3 μg/g, and the SRP concentration in the HCl-P_{TI} extract ranged from 1944.4 to 26,553.5 μg/L (Fig. 4). After PO_4 was enriched by the Zr-Oxide gel, the average enrichment rate of PO_4 in HCl-P_{TI} extract in other sites reached 95.3% except for the relatively lower enrichment rate of DCS site (86.1%). The lower enrichment rate of 86.1% was due to the higher SRP concentration and larger amounts of PO_4 in the sediment HCl-P_{TI} extract of the DCS site. With the increased number of Zr-Oxide gel or the enrichment time, a higher enrichment rate was achieved. In this study, the enrichment rates in the HCl-P_{TI} extract obtained from GHX and GLD site sediments were increased from 92.6% to 95.5%–100% because of the increasing number of Zr-Oxide gel and the enrichment time, respectively (Table 1). Within 1–3 days, the time required for the Zr-Oxide gel reached 90% of the PO_4 enrichment rate in the HCl-P_{TI} extract, indicating the PO_4 enrichment by Zr-Oxide gel to be a rapid process.

The amount of PO_4 eluted from the Zr-Oxide gel per unit area was between 13.9 and 179.3 μg P/cm^2, and the elution rate of PO_4 was between 91.6% and 100.4% (Table 1), suggesting that the PO_4 could be easily eluted from the Zr-Oxide gel. The SRP concentration in the HCl-P_{TI} extract was significantly positively correlated with the amount of PO_4 eluted from the Zr-Oxide gel per unit area ($R^2 = 0.9711$, $P < 0.01$, Figure S1). As the SRP concentration in HCl-P_{TI} extract increased, the Zr-Oxide gel showed a greater enrichment potential to PO_4. In summary, the Zr-Oxide gel has great advantages in the purification protocol for $\delta^{18}O_P$ analysis of HCl-P_{TI} in sediment and soil due to its efficient enrichment and elution of PO_4. This very simple operation can greatly simplify PO_4 purification operation which is cumbersome in the conventional methods for $\delta^{18}O_P$ analysis.

4.2. Effect of Zr-Oxide gel on simultaneous removal of various impurities in HCl-P_{TI} extracts

The HCl-P_{TI} extract contained a large number of metal ions, such as $Fe^{2+/}3^+$, Ca^{2+}, trace elements, and a high concentration of Cl^- (mainly from HCl itself), significantly interfering the subsequent $\delta^{18}O_P$ purification. For example, most metals can form the hydroxide precipitations, which affect the PO_4 enrichment and the removal of various impurities. If the large amount of Cl^- cannot be effectively removed, it will form the AgCl precipitate with Ag^+ to mix with the final Ag_3PO_4 solid. In addition to the lower simultaneous removal rates of SO_4^{2-} (85.9%) and K (71.6%), the simultaneous removal rate of other impurities by the Zr-Oxide gel was more than 96.2%, especially the removal rate of Cl^- was 99.9%. This high-efficiency and synchronous removal of impurities of HCl-P_{TI} extracts in a single step has significant advantages over the cumbersome multi-step removal of impurities in the previous methods, especially greatly simplifying the removal difficulty of Cl^- and metal ions, such as $Fe^{2+/3+}$, Ca^{2+} (Liu et al., 2019). Although a small amount of Zr is introduced when using the Zr-Oxide gel, the Zr can be removed by subsequent cation exchange resin and the final Ag_3PO_4 solid sample is not contaminated by Zr (Fig. 5).

4.3. The $\delta^{18}O_P$ fractionation discussion in PO_4 enrichment and elution by Zr-Oxide gel

Previous studies have proved that the enrichment and elution of PO_4 by Zr-Oxide gel is a reversible chemical equilibrium reaction process (Chitrakar et al., 2006; Ding et al., 2010). PO_4 can easily bind with the metal ions of the Zr-Oxide gel through covalent bonds to achieve the objective of enrichment. Under the alkaline condition, the chemical reaction equilibrium shifts in the reverse direction, and the PO_4 is easily eluted (Ding et al., 2010). It can be observed that the P–O bond of PO_4 doesn't break during the enrichment and elution process, thus, it can be inferred that the P–O bond would not cause $\delta^{18}O_P$ fractionation. Moreover, in this study, the Zr-Oxide gel exhibited a very high PO_4 enrichment and elution rate (close to 100%), also indicating that the PO_4 enrichment and elution would not cause significant $\delta^{18}O_P$ fractionation. Besides, in our previous studies, the $\delta^{18}O_P$ composition of water samples in the phosphate mining area was compared with the enriching and eluting PO_4 using the Zr-Oxide gel and the improved McLaughlin (2004) method, and the $\delta^{18}O_P$ compositions from these two methods had no significant difference, indicating that the Zr-Oxide gel does not cause the significant $\delta^{18}O_P$ fractionation during the enrichment and elution of PO_4 of HCl-P_{TI} in sediment and soil (Liu et al., 2021).

4.4. Advantages of the novel method for $\delta^{18}O_P$ analysis of HCl-P_{TI} in sediments and soils

The newly developed method in this study took advantage of the strong PO_4 enrichment ability of Zr-Oxide gel in acidic solution and the

significant advantage of simultaneous removal of most impurities. Zr-Oxide gel was used for the purification protocol for $\delta^{18}O_P$ analysis of HCl-P_{TI} in sediments and soils, which is not involved by previous methods. In particular, only a very small number of Zr-Oxide gels were required to selectively and efficiently enrich and elute the PO_4 and synchronously remove most of the various impurities in the HCl-P_{TI} extract from sediment or soil samples, and after several simplified further purification steps, the Ag_3PO_4 solid with high purity could be obtained for $\delta^{18}O_P$ composition analysis. On one hand, the new method greatly simplifies the cumbersome multi-step operations of enriching PO_4 and removing impurities, especially overcomes the difficulty of removing Cl^- completely in conventional methods (McLaughlin et al., 2004; Zohar et al., 2010), and also significantly reduces the economic and time costs. On the other hand, the new purification protocol can reduce the loss of PO_4 and improve the P recovery because of simplification of purification steps, and remarkably avoid the interference of many metal ions (such as $Fe^{2+/3+}$, Ca^{2+}, Table S1) which are easy to produce such as hydroxide precipitate and affect the purification of PO_4 in conventional methods. Besides, only less sample weight is needed in this new method, which is conducive to the $\delta^{18}O_P$ analysis for some sediment or soil samples that are difficult to obtain from the field.

5. Conclusion and prospect

In this study, a simple and reliable purification method for $\delta^{18}O_P$ analysis of HCl-P_{TI} in sediment and soil was developed based on the strong abilities of enrichment and elution of PO_4 and simultaneous removal of various impurities in acidic HCl-P_{TI} extract by Zr-Oxide gel. It was concluded that the Zr-Oxide gel could enrich and elute the PO_4 from the HCl-P_{TI} extract with complex chemical compositions, and the enrichment and elution rates of PO_4 could achieve 100%. Moreover, this method could also efficiently and synchronously remove impurities, such as anions, DOC, metals, and trace elements, and the removal rates of most impurities could be more than 96%, overcoming the limitations of tedious impurity removal in conventional methods, in particular, the removal rate of Cl^- reached 99.9%, simply and effectively solving the difficulty of Cl^- removal of HCl-P_{TI} extract. The high-purity Ag_3PO_4 solid could be obtained for $\delta^{18}O_P$ composition analysis.

In the future, this method would be extended to the $\delta^{18}O_P$ purification of the acid extract from different environmental samples, such as rocks, fossils, bones, and plants. The study provides a potential research direction for the purification protocol of $\delta^{18}O_P$ in complex systems with various chemical impurities.

CRediT authorship contribution statement

Yong Liu: Investigation, Conceptualization, Data curation, Writing - original draft, Visualization. Jingfu Wang: Methodology, Formal analysis, Writing -review & editing, Project administration. Haiquan Yang: Methodology, Writing - review & editing, Formal analysis. Shihao Jiang: Investigation, Data curation. Zuxue Jin: Investigation, Data curation. Jingan Chen: Methodology, Review & editing, Validation.

Declaration of competing interest

The authors declare that they have no known competing financial interests or personal relationships that could have appeared to influence the work reported in this paper.

Acknowledgments

This study is funded jointly by the National Natural Science Foundation of China (41907279, 41773145, 41977296), the Strategic Priority Research Program of Chinese Academy of Sciences (No. XDB40020400), the Chinese NSF Joint Fund Project (No. U1612441), the Youth Innovation Promotion Association CAS (2019389), the CAS Interdisciplinary Innovation Team.

Appendix A. Supplementary data

Supplementary data to this article can be found online at https://doi.org/10.1016/j.apgeochem.2021.104978.

References

Amelung, W., Antar, P., Kleeberg, I., Oelmann, Y., Lücke, A., Alt, F., Lewandowski, H., Pätzold, S., Barej, J.A.M., 2015. The $\delta^{18}O$ signatures of HCl-extractable soil phosphates: methodological challenges and evidence of the cycling of biological P in arable soil. Eur. J. Soil Sci. 66 (6), 965–972. https://doi.org/10.1111/ejss.12288.

Angert, A., Weiner, T., Mazeh, S., Sternberg, M., 2012. Soil phosphate stable oxygen isotopes across rainfall and bedrock gradients. Environ. Sci. Technol. 46, 2156–2162. https://doi.org/10.1021/es203551s.

Bate, D.B., Barrett, J.E., Poage, M.A., Virginia, R.A., 2008. Soil phosphorus cycling in an Antarctic polar desert. Geoderma 144 (1–2), 21–31. https://doi.org/10.1016/j.geoderma.2007.10.007.

Bi, Q.F., Zheng, B.X., Lin, X.Y., Li, K.J., Liu, X.P., Hao, X.L., Zhang, H., Zhang, J.B., Jaisi, D.P., Zhu, Y.G., 2018. The microbial cycling of phosphorus on long-term fertilized soil: insights from phosphate oxygen isotope ratios. Chem. Geol. 483, 56–64. https://doi.org/10.1016/j.chemgeo.2018.02.013.

Blake, R.E., O'Neil, J.R., Garcia, G.A., 1997. Oxygen isotope systematics of biologically mediated reactions of phosphate: I. Microbial degradation of organophosphorus compounds. Geochem. Cosmochim. Acta 61, 4411–4422. https://doi.org/10.1016/S0016-7037(97)00272-X.

Blake, R.E., Chang, S.J., Lepland, A., 2010. Phosphate oxygen isotopic evidence for a temperate and biologically active Archaean ocean. Nature 464, 1029–U1089. https://doi.org/10.1038/nature08952.

Burmann, F., Keim, M.F., Oelmann, Y., Teiber, H., Marks, M.A.W., Mark, G., 2013. The source of phosphate in the oxidation zone of ore deposits: evidence from oxygen isotope compositions of pyromorphite. Geochem. Cosmochim. Acta 123, 427–439. https://doi.org/10.1016/j.gca.2013.07.042.

Chang, S.J., Blake, R.E., 2015. Precise calibration of equilibrium oxygen isotope fractionations between dissolved phosphate and water from 3 to 37°C. Geochem. Cosmochim. Acta 150, 314–329. https://doi.org/10.1016/j.gca.2014.10.030.

Chen, Q., Chen, J., Wang, J., Guo, J., Jin, Z., Yu, P., Ma, Z., 2019. *In situ*, high-resolution evidence of phosphorus release from sediments controlled by the reductive dissolution of iron-bound phosphorus in a deep reservoir, southwestern China. Sci. Total Environ. 666, 39–45. https://doi.org/10.1016/j.scitotenv.2019.02.194.

Chitrakar, R., Tezuka, S., Sonoda, A., Sakane, K., Ooi, K., Hirotsu, T., 2006. Selective adsorption of phosphate from seawater and wastewater by amorphous zirconium hydroxide. J. Colloid Interface Sci. 297 (2), 426–433. https://doi.org/10.1016/j.jcis.2005.11.011.

Ding, S., Xu, D., Sun, Q., Yin, H., Zhang, C., 2010. Measurement of dissolved reactive phosphorus using the diffusive gradients in thin films technique with a high-capacity binding phase. Environ. Sci. Technol. 44 (21), 8169–8174. https://doi.org/10.1021/es1020873.

Ding, S., Jia, F., Xu, D., Sun, Q., Zhang, L., Fan, C., Zhang, C., 2011. High-resolution, two-dimensional measurement of dissolved reactive phosphorus in sediments using the diffusive gradients in thin films technique in combination with a routine procedure. Environ. Sci. Technol. 45 (22), 9680–9686. https://doi.org/10.1021/es202785p.

Ezzati, G., Fenton, O., Healy, M.G., Christianson, L., Feyereisen, G.W., Thornton, S., Chen, Q., Fan, B., Ding, J., Daly, K., 2020. Impact of P inputs on source-sink P dynamics of sediment along an agricultural ditch network. J. Environ. Manag. 257, 109988. https://doi.org/10.1016/j.jenvman.2019.109988.

Goldhammer, T., Brunner, B., Bernasconi, S., Ferdelman, T.G., Zabel, M., 2011. Phosphate oxygen isotopes: insights into sedimentary phosphorus cycling from the Benguela upwelling system. Geochem. Cosmochim. Acta 75, 3741–3756. https://doi.org/10.1016/j.gca.2011.04.006.

Gooddy, D.C., Lapworth, D.J., Ascott, M.J., Bennett, S.A., Heaton, T.H.E., Surridge, B.W. J., 2015. Isotopic fingerprint for phosphorus in drinking water supplies. Environ. Sci. Technol. 49, 9020–9028. https://doi.org/10.1021/acs.est.5b01137.

Granger, S.J., Harris, P., Peukert, S., Guo, R., Tamburini, F., Blackwell, M.S.A., Howden, N.J.K., McGrath, S., 2017. Phosphate stable oxygen isotope variability within a temperate agricultural soil. Geoderma 285, 64–75. https://doi.org/10.1016/j.geoderma.2016.09.020.

Guo, M., Li, X., Song, C., Liu, G., Zhou, Y., 2020. Photo-induced phosphate release during sediment resuspension in shallow lakes: a potential positive feedback mechanism of eutrophication. Environ. Pollut. 258, 113679. https://doi.org/10.1016/j.envpol.2019.113679.

Helfenstein, J., Tamburini, F., von Sperber, C., Massey, M.S., Pistocchi, C., Chadwick, O. A., Vitousek, P.M., Kretzschmar, R., Frossard, E., 2018. Combining spectroscopic and isotopic techniques gives a dynamic view of phosphorus cycling in soil. Nature communication 9, 3226. https://doi.org/10.1038/s41467-018-05731-2.

Ide, J., Ishida, T., Cid-Andres, A.P., Osaka, K., Iwata, T., Hayashi, T., Akashi, M., Tayasu, I., Paytan, A., Okuda, N., 2020. Factors characterizing phosphate oxygen isotope ratios in river water: an inter-watershed comparison approach. Limnology 21, 365–377. https://doi.org/10.1007/s10201-020-00610-6.

Ishida, T., Uehara, Y., Iwata, T., Cid-Andres, A.P., Asano, S., Ikeya, T., Osaka, K., Ide, J., Privaldos, O.L.A., De Jesus, I.B.B., Peralta, E.M., Triño, E.M.C., Ko, C.Y., Paytan, A., Tayasu, I., Okuda, N., 2019. Identification of phosphorus sources in a watershed

using a phosphate oxygen isoscape approach. Environ. Sci. Technol. 53, 4707–4716. https://doi.org/10.1021/acs.est.8b05837.
Jaisi, D.P., Blake, R.E., 2010. Tracing sources and cycling of phosphorus in Peru Margin sediments using oxygen isotopes in authigenic and detrital phosphates. Geochem. Cosmochim. Acta 74, 3199–3212. https://doi.org/10.1016/j.gca.2010.02.030.
Jaisi, D.P., Kukkadapu, R.K., Stout, L.M., Varga, T., Blake, R.E., 2011. Biotic and abiotic pathways of phosphorus cycling in minerals and sediments: insights from oxygen isotope ratios in phosphate. Environ. Sci. Technol. 45 (15), 6254–6261. https://doi.org/10.1021/es200456e.
Jin, X.C., Wang, S.R., Pang, Y., Wu, F.C., 2006. Phosphorus fractions and the effect of pH on the phosphorus release of the sediments from different trophic areas in Taihu Lake, China. Environ. Pollut. 139, 288–295. https://doi.org/10.1016/j.envpol.2005.05.010.
Joshi, S., Li, W., Bowden, M., Jaisi, D.P., 2018. Sources and pathways of formation of recalcitrant and residual phosphorus in an agricultural soil. Soil Systems 2 (3), 45. https://doi.org/10.3390/soilsystems2030045.
Koch, M., Kruseb, J., Eichler-Lőbermannc, B., Zimmer, D., Willbold, S., Leinweber, P., Siebers, N., 2018. Phosphorus stocks and speciation in soil profiles of a long-term fertilizer experiment: evidence from sequential fractionation, P *K*-edge XANES, and ^{31}P NMR spectroscopy. Geoderma 316, 115–126. https://doi.org/10.1016/j.geoderma.2017.12.003.
Kwak, D.H., Jeon, Y.T., Hur, Y.D., 2018. Phosphorus fractionation and release characteristics of sediment in the Saemangeum Reservoir for seasonal change. Int. J. Sediment Res. 33, 250–261. https://doi.org/10.1016/j.ijsrc.2018.04.008.
Liang, Y., Blake, R.E., 2006. Oxygen isotope signature of Pi regeneration from organic compounds by phosphomonoesterases and photooxidation. Geochem. Cosmochim. Acta 70, 3957–3969. https://doi.org/10.1016/j.gca.2006.04.036.
Liang, Y., Blake, R.E., 2009. Compound- and enzyme-specific phosphodiester hydrolysismechanisms revealed by δ^{18}O of dissolved inorganic phosphate: implications for marine P cycling. Geochem. Cosmochim. Acta 73, 3782–3794. https://doi.org/10.1016/j.gca.2009.01.038.
Liu, Y., Wang, J., Chen, J., Zhang, R., Ji, Y., Jin, Z., 2019. Pretreatment method for the analysis of phosphate oxygen isotope ($\delta^{18}O_P$) of different phosphorus fractions in freshwater sediments. Sci. Total Environ. 685, 229–238. https://doi.org/10.1016/j.scitotenv.2019.05.238.
Liu, Y., Wang, J., Chen, J., Jin, Z., Ding, S., Yang, X., 2021. Method for phosphate oxygen isotopes analysis in water based on *in situ* enrichment, elution, and purification. J. Environ. Manag. 111618 https://doi.org/10.1016/j.jenvman.2020.111618.
Longinelli, A., Nuti, S., 1973. Revised phosphate-water isotopic temperature scale. Earth Planet Sci. Lett. 19 (3), 373–376. https://doi.org/10.1016/0012-821X(73)90088-5.
McLaughlin, K., Silva, S., Kendall, C., Stuart-Williams, H., Paytan, A., 2004. A precise method for the analysis of δ^{18}O of dissolved inorganic phosphate in seawater. Limnol Oceanogr. Methods 2, 202–212. https://doi.org/10.4319/lom.2004.2.202.
McLaughlin, K., Kendall, C., Silva, S.R., Young, M., Paytan, A., 2006. Phosphate oxygen isotope ratios as a tracer for sources and cycling of phosphate in North San Francisco Bay, California. J. Geophys. Res. 111 https://doi.org/10.1029/2005JG000079. G030003, 1-12.
McLaughlin, K., Sohm, J.A., Cutter, G.A., Lomas, M.W., Paytan, A., 2013. Phosphorus cycling in the Sargasso Sea: Investigation using the oxygen isotope composition of phosphate, enzyme-labeled fluorescence, and turnover times. Global Biogeochem. Cycles 27, 375–387. https://doi.org/10.1002/gbc.20037.
Mingus, K.A., Liang, X.M., Massoudieh, A., Jaisi, D.P., 2019. Stable isotopes and bayesian modeling methods of tracking sources and differentiating bioavailable and recalcitrant phosphorus pools in suspended particulate matter. Environ. Sci. Technol. 53, 69–76. https://doi.org/10.1021/acs.est.8b05057.
Murphy, J., Riley, J.P., 1962. A modified single solution method for the determination of phosphate in natural water. Anal. Chim. Acta 27, 31–36. https://doi.org/10.1016/S0003-2670(00)88444-5.
Paytan, A., Kolodny, Y., Neori, A., Luz, B., 2002. Rapid biologically mediated oxygen isotope exchange between water and phosphate. Global Biogeochem. Cycles 16 (1), 13-1-13-8. https://doi.org/10.1029/2001GB001430.
Paytan, A., Roberts, K., Watson, S., Peek, S., Chuang, P.C., Defforey, D., Kendall, C., 2017. Internal loading of phosphate in Lake Erie Central Basin. Sci. Total Environ. 259, 1356–1365. https://doi.org/10.1016/j.scitotenv.2016.11.133.
Pfahler, V., Macdonald, A., Mead, A., Smith, A.C., Tamburini, F., Blackwell, M.S.A., Granger, S.J., 2020. Changes of oxygen isotope values of soil P pools associated with changes in soil pH. Sci. Rep. 10, 2065. https://doi.org/10.1038/s41598-020-59103-2.
Pistocchi, C., Tamburini, F., Gruau, G., Ferhi, A., Trevisan, D., Dorioz, J.M., 2017. Tracing the sources and cycling of phosphorus in river sediments using oxygen isotopes: methodological adaptations and first results from a case study in France. Water Res. 111, 346–356. https://doi.org/10.1016/j.watres.2016.12.038.
Pu, J., Ni, Z., Wang, S., 2020. Characteristics of bioavailable phosphorus in sediment and potential environmental risks in Poyang Lake: the largest freshwater lake in China. Ecol. Indicat. 115, 106409. https://doi.org/10.1016/j.ecolind.2020.106409.
Reina, M., Espinar, J.L., Serrano, L., 2006. Sediment phosphate composition in relation to emergent macrophytes in the Doñana Marshes (SW Spain). Water Res. 40, 1185–1190. https://doi.org/10.1016/j.watres.2006.01.031.
Sun, Q., Chen, J., Wang, J., Yang, H., Ji, Y., Lan, C., Wang, X., 2017. High-resolution distribution characteristics of phosphorous, iron and sulfur across the sediment-water interface of Aha Reservoir. Environ. Sci. 38 (7), 2810-2018 https://doi.org/10.13227/j.hjkx.201611159 (In Chinese with English Abstract).
Tamburini, F., Bernasconi, S.M., Angert, A., Weiner, T., Frossard, E., 2010. A method for the analysis of the δ^{18}O of inorganic phosphate extracted from soils with HCl. Eur. J. Soil Sci. 61 (6), 1025–1032. https://doi.org/10.1111/j.1365-2389.2010.01290.x.
Tamburini, F., Pfahler, V., Bunemann, E.K., Guelland, K., Bernasconi, S.M., Frossard, E., 2012. Oxygen isotopes unravel the role of microorganisms in phosphate cycling in soils. Environ. Sci. Technol. 46, 5956–5962. https://doi.org/10.1021/es300311h.
Tamburini, F., Pfahler, V., von Sperber, C., Frossard, E., 2014. Oxygen isotopes for unraveling phosphorus transformations in the soil-plant system: a review. Soil Sci. Soc. Am. J. 78, 38–46. https://doi.org/10.2136/sssaj2013.05.0186dgs.
Tian, L., Guo, Q., Yu, G., Zhu, Y., Lang, Y., Wei, R., Hu, J., Yang, X., Ge, T., 2020. Phosphorus fractions and oxygen isotope composition of inorganic phosphate in typical agricultural soils. Chemosphere 239, 124622. https://doi.org/10.1016/j.chemosphere.2019.124622.
Walker, T.W., Syers, J.K., 1976. The fate of phosphorus during pedogenesis. Geoderma 15 (1), 1–19. https://doi.org/10.1016/0016-7061(76)90066-5.
Wang, F., Liu, C., Liang, X., Wei, Z., 2003. Microbial activity at the sediment-water interface and its influence on remigration and enrichment of trace elements in Aha Lake, Guizhou province, China. Chin. Sci. Bull. 48 (19), 2073–2078. https://doi.org/10.3321/j.issn:0023-074X.2003.19.014 (In Chinese).
Wang, J., Chen, J., Jin, Z., Guo, J., Yang, H., Zeng, Y., Liu, Y., 2020. Simultaneous removal of phosphate and ammonium nitrogen from agricultural runoff by amending soil in lakeside zone of Karst area, Southern China. Agric. Ecosyst. Environ. 289, 106745. https://doi.org/10.1016/j.agee.2019.106745.
Weiner, T., Mazeh, S., Tamburini, F., Frossard, E., Bernasconi, S.M., Chiti, T., Angert, A., 2011. A method for analyzing the δ^{18}O of resin-extractable soil inorganic phosphate. Rapid Commun. Mass Spectrom. 25 (5), 624–628. https://doi.org/10.1002/rcm.4899.
Yuan, H., Li, Q., Kukkadapu, R.K., Liu, E., Yu, J., Fang, H., Li, H., Jaisi, D.P., 2019. Identifying sources and cycling of phosphorus in the sediment of a shallow freshwater lake in China using phosphate oxygen isotopes. Sci. Total Environ. 676, 823–833. https://doi.org/10.1016/j.scitotenv.2019.04.322.
Zhang, H., Shi, L., Lu, H., Shao, Y., Liu, S., Fu, S., 2020. Drought promotes soil phosphorus transformation and reduces phosphorus bioavailability in a temperate forest. Sci. Total Environ. 732, 139295. https://doi.org/10.1016/j.scitotenv.2020.139295.
Zhu, Y., Wu, F., Liu, Y., Wei, Y., Liu, S., Feng, W., Giesy, J.P., 2017. Microbial biomass and community composition involved in cycling of organic phosphorus in sediments of Lake Dianchi, Southwest China. Geomicrobiol. J. 34 (3), 249–260. https://doi.org/10.1080/01490451.2016.1184726.
Zohar, I., Shaviv, A., Klass, T., Roberts, K., Paytan, A., 2010. Method for the analysis of oxygen isotopic composition of soil phosphate fractions. Environ. Sci. Technol. 44 (19), 7583–7588. https://doi.org/10.1021/es100707f.